16. MAGNETIC PROPERTIES OF BASALTS FROM THE CENTRAL NORTH ATLANTIC OCEAN[1]

Guy M. Smith and Subir K. Banerjee, Department of Geology and Geophysics, University of Minnesota[2]

ABSTRACT

The magnetic properties of 56 samples of basalt from DSDP Leg 82 were studied in order to examine regional variations as well as the general question of the origin or remanence. Magnetization was carried, for the most part, by typical low temperature oxidized titanomagnetites, although two samples did show anomalous thermomagnetic curves. The natural remanence is distinctly different from an anhysteretic remanent magnetization and is hypothesized (by inference) to also be different from a thermoremanent magnetization (TRM) also. This suggests that alteration not only reduces the initial TRM but also changes it to chemical remanent magnetization with a significantly different magnetic character. An examination of thermomagnetic data tentatively suggests that the ulvospinel content of the titanomagnetites may be more variable than is commonly assumed. With the exception of a slight increase in saturation magnetization with decreasing latitude, no significant regional variations were evident.

INTRODUCTION

This paper reports on the magnetic properties of 56 samples of basalt from eight of the nine sites drilled on DSDP Leg 82 (no significant amount of basalt was recovered from Site 560). These sites were distributed over a fairly broad area and thus offer an opportunity to study the extent to which magnetic properties of the upper basement vary horizontally.

We measured a number of magnetic parameters including:

1. intensity, direction, and stability of natural remanent magnetization (NRM);
2. weak field susceptibility (χ_0).
3. hysteresis loop parameters, i.e., saturation magnetization, J_s; saturation remanence, J_{rs}; coercivity, H_c; remanent coercivity, H_{cr}; and paramagnetic susceptibility, χ_p.
4. Curie temperature, T_c, and thermomagnetic curve analysis; and
5. intensity and stability of anhysteretic remanent magnetization (ARM).

METHODS

Magnetic remanence measurements were made on a Schonstedt spinner magnetometer. Alternating field (AF) demagnetization was performed on a single axis Schonstedt demagnetizer. Each step was repeated for three orthogonal directions to ensure complete demagnetization. For ARM induction, we also used this instrument with a 0.5 Oe static bias field and a peak AF field (coaxial) of 1000 Oe.

Hysteresis loops were obtained with a Princeton Applied Research vibrating sample magnetometer coupled to an x-y recorder. Thermomagnetic measurements were also made on this instrument with an automatically controlled heating rate (20°C/minute) in a vacuum of better than 10^{-6} torr. Temperature calibration is based on measurements of pure Ni (T_c = 358°C) and pure Fe_3O_4 (T_c = 580°C). Values are obtained with the graphical method (Moskowitz, 1981).

Weak field susceptibility was measured with a Conservation Instruments ("Bartington") bridge.

RESULTS

Natural Remanent Magnetization

NRM intensities vary from 7.74×10^{-3} to 1.77×10^{-4} emu·cm^{-3}. Average values for each site and rock type are given in Table 1 (details are in Appendix A at the end of this chapter). With the exceptions of Sites 557 and 559, the site-averaged values are fairly close. Site 557 is slightly high but this is based on only two samples, which may not be representative. Site 559 is quite low but, again, the data represent only four samples and may be misleading. The first six sites have higher NRM intensities for pillow interiors than margins but the reverse is true for Sites 563 and 564. Flow interiors are also more strongly magnetized than margins with the exception of Site 562. Although these may be trends in these data, their validity seems questionable and no attempt to discover possible trends will be made here.

Median demagnetizing fields (MDF_N) run quite high generally with many in excess of 400 Oe and several above 1000 Oe. The notable exception is Site 559 with MDF's of 99 and 113 Oe. Hole 558 flow and pillow margins tend to have a somewhat higher MDF than their respective interiors, but otherwise no pattern is apparent.

Samples frequently have a small (<10%) low coercivity component (<100 Oe), which is generally steep and positive. Much of this is probably the result of relatively recent viscous remanence. Some have nearly vertical inclinations, but this may be an artifact of drilling. As these components are generally small and easily demagnetized, they represent no significant problem.

A few samples show multicomponent behavior persisting to such large fields that a stable secondary remanence is probable (see Appendix A). The difference in inclination is large enough so that magnetization must have been acquired in two or more episodes separated by tectonic rotation and/or a sufficient time lapse for

[1] Bougault, H., Cande, S. C., et al., *Init. Repts. DSDP*, 82: Washington (U.S. Govt. Printing Office).

[2] Address: Department of Geology and Geophysics, University of Minnesota, Minneapolis, Minnesota 55455.

Table 1. Natural remanent magnetization (NRM) values (in emu/cm^3).

Hole	Pillows		Flows		Average
	Margin	Interior	Margin	Interior	
556	1.27×10^{-3}	3.53×10^{-3}	2.20×10^{-3}	3.94×10^{-3}	3.04×10^{-3}
557					7.59×10^{-3}
558	8.84×10^{-4}	2.66×10^{-3}	8.88×10^{-4}	5.30×10^{-3}	2.20×10^{-3}
559	4.32×10^{-4}	5.87×10^{-4}			5.10×10^{-4}
561	2.35×10^{-3}	3.31×10^{-3}		2.22×10^{-3}	2.53×10^{-3}
562	1.32×10^{-3}	2.34×10^{-3}	2.00×10^{-3}	1.40×10^{-3}	1.85×10^{-3}
563	4.96×10^{-3}	1.95×10^{-3}			3.46×10^{-3}
564	4.46×10^{-3}	2.12×10^{-3}	1.68×10^{-3}	2.91×10^{-3}	2.78×10^{-3}
Average	2.79×10^{-3}	2.36×10^{-3}	1.65×10^{-3}	3.15×10^{-3}	3.00×10^{-3}

Note: Samples that could not be assigned to a particular rock type were included in the final averages.

the field to change significantly (1000 yr. or so). This phenomenon seems a local one; nearby samples with otherwise similar characteristics show no such behavior. Multicomponent remanence does not seem to be associated with any particular rock type.

Koenigsberger ratios were generally large, usually in excess of 10 and often much higher.

Hystersis Loop Parameters

Hysteresis loop parameters provide a measure of the intrinsic magnetic properties of the samples and are useful in studying the origin of remanence. They are given in Appendix B at the end of this chapter.

Saturation magnetization, J_s, is a measure of the total amount of magnetic material present (if the composition is known, it is an exact measure). Average values of J_s are given in Table 2. With the exception of Sites 562 and 563, the variation of J_s between rock types is similar to that of J_N and suggests that the primary cause of variation in remanence is simply the amount of magnetic carrier present. There appears to be an increase in J_s as the latitude decreases, although the small number of sites precludes any meaningful statistical test.

Coercivity, H_c, is similar, though not identical, to the MDF as a measure of magnetic stability. Figure 1A shows a comparison of H_c and MDF_N and Figure 1B shows H_c and MDF_A. As can be seen, there is substantially less scatter for H_c-MDF_A graph. This is one piece of evidence (to be discussed later) that ARM and NRM are significantly different in these samples.

The two ratios, J_{rs}/J_s and H_{cr}/H_c, are commonly interpreted as indicators of domain state (Day et al., 1977). The values for these samples suggest that they contain predominantly single-domain or small pseudo-single domain grains with sizes of a few microns at most. An alternate possibility is that the sample contains larger (10–20 μm) grains that are in a metastable single-domain state (Halgedahl and Fuller, 1983). Future polished section work should help clarify this issue.

Curie Temperature

The Curie temperature, T_c, is the temperature below which a magnetic material becomes magnetically ordered. The value for titanomagnetites is very sensitive to both Ti content (usually expressed as the proportion of ulvospinel to magnetite) and degree of low temperature oxidation (Syono, 1965; Readman and O'Reilly, 1972; Moskowitz and Banerjee, 1981). Generally, T_c decreases with increasing Ti content and increases with oxidation. When a low temperature oxidized titanomagnetite (titanomaghemite) is heated, it produces the characteristic thermomagnetic curve seen in Figure 2A. The second maximum is due to the fact that titanomaghemite is metastable and inverts upon heating to a two-phase mixture with compositions close to magnetite and ilmenite. This causes a large difference in T_c measured from the heating and cooling curves, as well as a marked increase in magnetization.

There were only a few exceptions to the above pattern. Two samples had an initial T_c greater than 450°C

Table 2. Saturation magnetization (J_S) values (in $emu \cdot g^{-1}$).

Hole	Pillows		Flows		Average
	Margin	Interior	Margin	Interior	
556	5.86×10^{-2}	1.19×10^{-1}	6.13×10^{-2}	1.05×10^{-1}	8.78×10^{-2}
557					1.48×10^{-1}
558	8.43×10^{-2}	1.48×10^{-1}	7.82×10^{-2}	1.44×10^{-1}	1.11×10^{-1}
559	7.18×10^{-2}	9.66×10^{-2}			8.41×10^{-2}
561	2.80×10^{-1}	3.16×10^{-1}		3.00×10^{-1}	2.99×10^{-1}
562	2.57×10^{-1}	1.67×10^{-1}	3.83×10^{-1}	2.77×10^{-1}	2.45×10^{-1}
563	2.66×10^{-1}	3.24×10^{-1}			2.95×10^{-1}
564	3.17×10^{-1}	2.00×10^{-1}	1.05×10^{-1}	3.72×10^{-1}	2.56×10^{-1}
Average	1.91×10^{-1}	1.96×10^{-1}	1.57×10^{-1}	2.40×10^{-1}	1.99×10^{-1}

Note: Samples that could not be assigned to a particular rock type were included in the final averages.

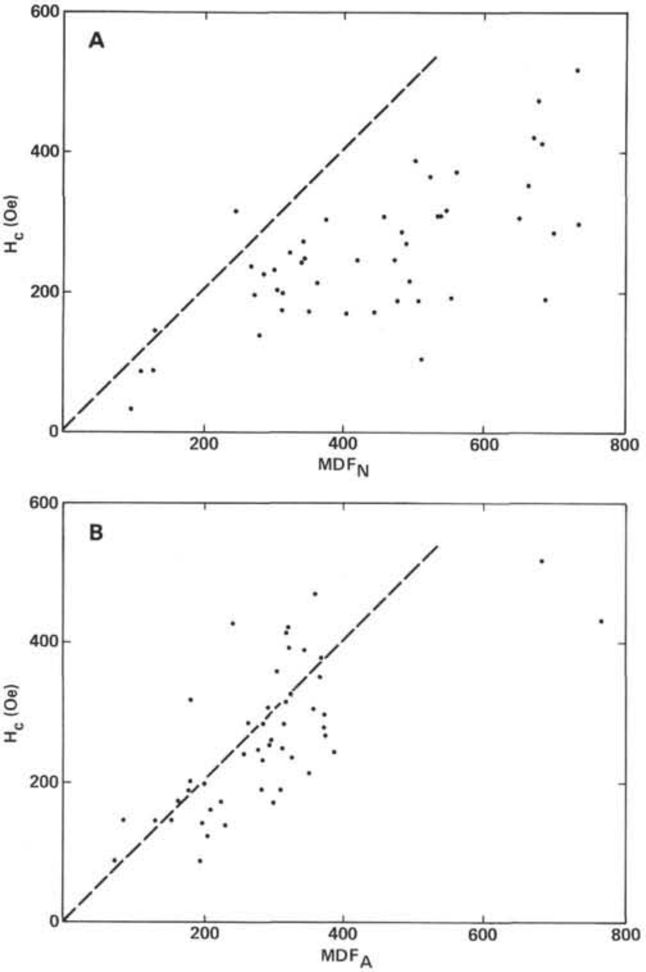

Figure 1. A. Coercivity (H_c) versus mean demagnetizing field for natural remanent magnetization (MDF_N). B. Coercivity (H_c) versus mean demagnetizing field for anhysteretic remanent magnetization (MDF_A).

(556-8-2, 80–83 cm and 564-6-2, 104–107 cm). Both were pillow margins and may have been partially deuterically altered at high temperature. Two other samples (561-3-1, 67–70 cm and 562-5-2, 104–107 cm) have somewhat unusual curves (Fig. 2B) with normal heating portions but apparently very low T_c cooling curves. We have, as yet, no explanation for this odd behavior, although reduction caused by presence of sulfides is a possibility. Two samples (557-1-1, 46–49 cm and 562-1-2, 27–30 cm) had very low T_c values and appear to be relatively unaltered.

Averages for the remaining more or less normal samples are given in Table 3. Pillow margins have consistently higher T_c suggesting that they are more altered than their interiors. The same is true for flows, with the exception of Site 562. There seems to be a general trend towards higher T_c's for older rocks but it is not very well defined.

It has been commonly accepted that the ulvospinel content of marine titanomagnetites is relatively constant (Johnson, 1979), although Steiner (1982) suggests that more variability may exist. Unfortunately, this is a difficult question to approach experimentally because the

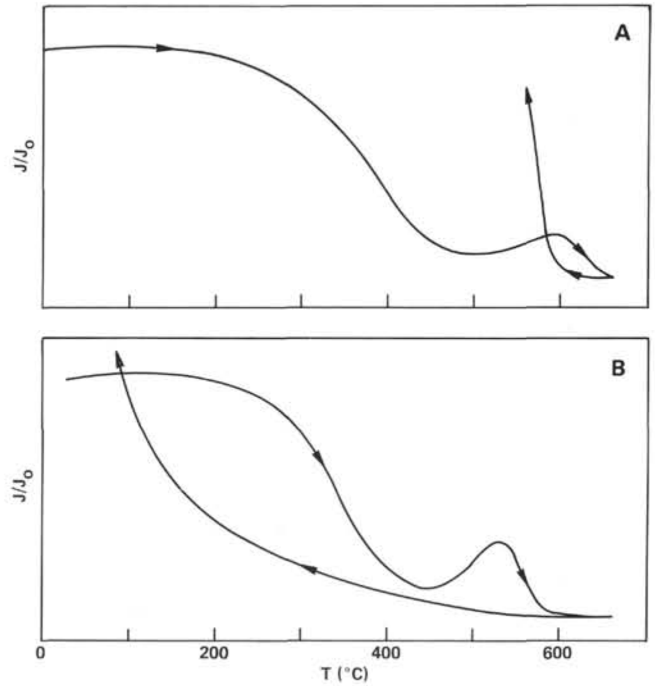

Figure 2. A. Thermomagnetic curve for a typical low temperature oxidized basalt (Sample 556-8-2, 6-9 cm). B. Atypical thermomagnetic curve (Sample 571-3-1, 67-70 cm) shown by two samples. Vertical axis is the relative magnetization (J/J_0) in arbitrary units. Horizontal axis (temperature) is uncorrected for instrumental offset (actual values are somewhat lower).

Table 3. Initial Curie temperatures (T_c) in °C.

	Pillows		Flows		
Hole	Margin	Interior	Margin	Interior	Average
556	405	325	365	340	357
557					273
558	353	297	328	313	325
559	355	338			346
561	375	335		323	339
562	260	275	265	338	284
563	414				415
564	423	335	365	285	321
Average	369	318	331	320	333

Note: Samples that could not be assigned to a particular rock type were included in the final averages.

grains that carry much of the remanence are too small for direct measurement of their composition (e.g., by electron microprobe). Curie points are governed by both composition and oxidation state and hence are ambiguous. One way to circumvent this problem is suggested by O'Reilly (1983) who shows that for his synthetic $x = 0.6$ titanomaghemites, there is a definite relationship between oxidation state (or T_c) and the ratio of J_s before inversion to that after inversion (J_f/J_i). All of our samples were heated well beyond the inversion temperature (~350°C, O'Reilly, 1983) in the process of measuring T_c (maximum temperature was about 620°C). Although the heating runs were relatively rapid (20°C/min), reruns of several samples showed little or no additional change in J_s, indicating that the bulk of the inversion process was complete after the first heating. Figure 3 shows our data along with the trend from O'Reilly (1983). Two things are immediately obvious; (1) there is no trend and (2) most of our values exceed those of O'Reilly, some by a substantial amount.

It is possible that there are some differences in the way in which the samples were inverted but this seems unlikely. Maximum temperatures were close to those of O'Reilly, and variations in vacuum and the possible presence of reducing agents do not seem sufficient to produce large discrepancies, although this matter needs further study. One factor that may contribute to the scatter of the data is variability in oxidation state among the various titanomaghemite grains in a sample; T_c tends to reflect the most oxidized grains, whereas J_f/J_i includes the whole assemblage. This mechanism does not, however, explain the large values of J_f/J_i relative to O'Reilly's results. We can find two possible explanations (not mutually exclusive) that could account for this discrepancy. One is that the seafloor oxidation process differed significantly from that to which O'Reilly's samples were exposed. The other is that the compositions of oceanic titanomagnetites are not as constant as has been commonly assumed. In all probability, two, or even all three, of these possible factors are present along with others that are less obvious. Further work is clearly necessary to resolve this issue.

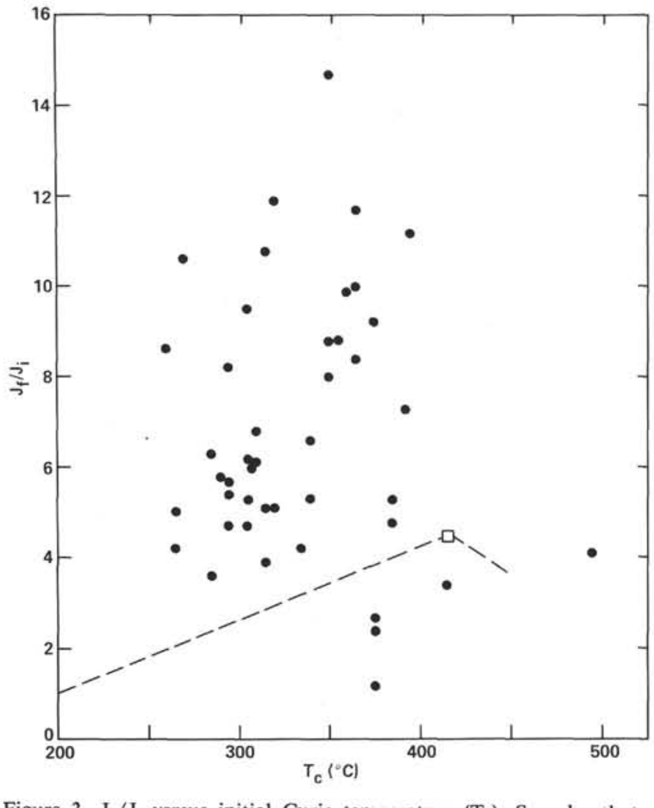

Figure 3. J_f/J_i versus initial Curie temperature (T_c). Samples that showed no sign of inversion were not included. J_f is saturation magnetization after inversion; J_i is saturation magnetization before inversion. The dashed line shows the trend of data from O'Reilly (1983).

Anhysteretic Remanent Magnetization

ARM is often used as a model for thermoremanent magnetization (TRM) because it does not require heating and consequent alteration of the sample. Levi and Merrill (1976) found that ARM intensity is usually less than TRM by a factor that varies but is generally greater than two (the exceptions were two large single crystals of magnetite that are not comparable to these samples). They also found that ARM and TRM had very similar AF demagnetization curves. In order to study the effect of low temperature oxidation on the original TRM, all samples were given an ARM, which was subsequently AF demagnetized. If the remanence is still essentially the original TRM, one would expect that the ARM intensity (J_A) would be less than half of the NRM value (J_N), and the median demagnetizing fields (MDF_A and MDF_N, respectively) should be about equal. This is generally not the case with our samples. J_A/J_N is greater than 0.5 in most cases, sometimes much greater (e.g., 559-6-2, 50–53 cm), and MDF_A/MDF_N generally is significantly less than 1.0 (Appendix A).

There are several sources of uncertainty in this comparison that should be considered in interpreting these data. J_A is a function of the inducing field and hence may be different from the actual field in which magnetization took place. However, it should be within, at most, ±50%. The MDF is not very sensitive to inducing field, and that comparison is probably reasonably accurate. Multicomponent remanence tends to produce an apparently harder demagnetization curve (i.e., greater MDF) than a comparable single component (this is a result of the geometry of vector demagnetization curves and has nothing to do with intrinsic magnetic properties). This effect is generally small and is not found in all samples in any case. Often a significant portion of the NRM is left at 1000 Oe (the limit of our machine). MDF_A would then only reflect the portion of the grains that can be affected by 1000-Oe fields and would be somewhat lower than MDF_N. This difference is easily corrected for, however, and is not sufficient to eliminate the disparity in MDF in many, if not most, samples. The comparison of results with those of Levi and Merrill (1976) may not be valid. They worked with pure magnetite, and only one of their samples was in the single-domain size range found for most (though not all) of the Leg 82 rocks (note that this sample had J_A/J_N = 0.24 and MDF_A/MDF_N = 1.2). Although further work is necessary, the consistency of their results suggests that more directly comparable samples would show similar behavior.

All factors taken into consideration, many, if not most, of the samples still seem to show distinctly different behaviors for NRM and ARM (and presumably TRM). It is well known that oxidation tends to decrease remanence and increase stability relative to their original values (e.g., Johnson, 1979). We tentatively conclude from these data that oxidation also causes these same changes relative to intrinsic (oxidized) magnetic parameters. This behavior suggests that we are not simply seeing a reduction in TRM but, in fact, its replacement by a chemical remanence with entirely different character, as in fact suggested by Hall (1977) on somewhat different grounds. Unfortunately, these data tell us nothing about possible effects on the direction of remanence.

SUMMARY

In general, these basalts are very similar to other such rocks recovered by DSDP. The most notable distinction was that they were unusually stable magnetically. Although they span a broad area of seafloor, they show no substantial trends either with latitude or age; however, there appears to be a small increase in J_s with decreasing latitude. The remanence appears to be dominated by a chemical remanent magnetization produced by low temperature alteration of the original TRM-bearing titanomagnetites. This remanence seems to be distinctly different from what would exist if the samples could be given a TRM in their oxidized state, having a lesser remanence and a greater stability. Nevertheless, the validity of the ARM-TRM analogy remains to be confirmed. There is also some evidence that the Ti content of the titanomagnetites may be more variable than often supposed. This too will require further study.

ACKNOWLEDGMENTS

We would like to thank Wendy Tormanen and Yvonne Meeks for their assistance with some of the measurements. Valuable assistance was also rendered on many occasions by Jim Marvin. We would also like to thank our reviewers, S. Beske-Diehl, B. Moskowitz, and R. Merrill, for many helpful comments and criticisms. This work was performed under NSF Grants OCE-8018692 and OCE-8214652.

REFERENCES

Day, R., Fuller, M.D., and Schmidt, V. A., 1977. Hysteresis properties of titanomagnetites: grain size and composition dependence. *Phys. Earth Planet. Inter.*, 13:260.

Halgedahl, S., and Fuller, M. D., 1983. The dependence of magnetic domain structure upon magnetization state with emphasis upon nucleation as a mechanism for pseudo-single-domain behavior. *J. Geophys. Res.*, 88:6505–6522.

Hall, J. M., 1977. Does TRM occur in oceanic layer 2 basalts? *J. Geomagn. Geoelectr.*, 29:411–420.

Johnson, H.P., 1979. Magnetization of the oceanic crust. *Rev. Geophys. Space Phys.*, 17:215–226.

Levi, S., and Merrill, R. T., 1976. A comparison of ARM and TRM in magnetite. *Earth Planet. Sci. Lett.*, 32:171–184.

Moskowitz, B. M., 1981. Methods for estimating Curie temperatures of titanomagnetites from experimental J_s-T data. *Earth Planet. Sci. Lett.*, 53:84–88.

Moskowitz, B. M., and Banerjee, S. K., 1981. Magnetic properties of synthetic titanomaghemites and some oceanic basalts. *J. Geophys. Res.*, 86:11869–11882.

O'Reilly, W., 1983. The identification of titanomaghemites: model mechanisms for the maghemitization and inversion processes and their magnetic consequences. *Phys. Earth Planet. Sci.*, 31:65–76.

Readman, P. W., and O''Reilly, W. O., 1972. Magnetic properties of oxidized (cation deficient) titanomagnetites $(Fe,Ti,\square)_3O_4$. *J. Geomagn. Geoelectr.*, 24:69–90.

Steiner, M., 1982. An investigation of ulvospinel composition and cation migration during maghemitization in Deep Sea Drilling Project Leg 61 titanomagnetites. *J. Geophys. Res.*, 87:5361–5374.

Syono, Y., 1965. Magnetocrystalline anisotropy and magnetostriction of Fe_3O_4-Fe_2TiO_4 series, with special application to rock magnetization. *Jpn. J. Geophys.*, 4:71–142.

Date of Initial Receipt: 31 May 1983
Date of Acceptance: 16 November 1983

APPENDIX A
Remanent Properties

Core-Section (interval in cm)	J_N (emu·cm^{-3})	I (°)	MDF_N (Oe)[a]	J_A (emu/cm^3)	MDF_A (Oe)	J_A/J_N	MDF_A/MDF_N	χ_0 (emu·cm^{-3}·Oe^{-1})	Q	Description
Hole 556										
5-1, 78-80	4.01×10^{-3}	−31	562	2.04×10^{-3}	371	0.51	0.66	8.29×10^{-5}	96.7	Pillow interior
5-1, 111-113	1.27×10^{-3}	−35[b]	675	1.96×10^{-3}	323	1.54	0.48	9.98×10^{-5}	25.5	Pillow margin
7-1, 47-49	2.02×10^{-3}	−25	274	2.42×10^{-3}	200	1.20	0.73	1.41×10^{-4}	28.7	Flow margin
7-3, 18-21	6.36×10^{-4}	−30	315	2.30×10^{-3}	200	3.59	0.63	1.11×10^{-4}	11.5	Flow interior
8-2, 6-9	3.05×10^{-3}	−38	481	2.02×10^{-3}	374	0.66	0.78	1.50×10^{-4}	40.7	Pillow interior
9-1, 143-146	7.24×10^{-4}	−6[b]	540	1.26×10^{-3}	297	1.73	0.55	1.04×10^{-4}	13.9	Flow interior
Average	1.95×10^{-3}	−28	475	1.96×10^{-3}	294	1.54	0.64	1.15×10^{-4}	36.2	
Hole 557										
1-1, 46-49	4.38×10^{-3}	−55	99	7.34×10^{-3}	34	1.68	0.34	2.76×10^{-3}	3.2	Basalt
1-1, 120-123	1.08×10^{-2}	−46	113	5.96×10^{-3}	74	0.55	0.65	1.05×10^{-3}	20.6	Basalt
Average	7.59×10^{-3}	−51	106	6.52×10^{-3}	54	1.12	0.50	1.19×10^{-3}	11.9	
Hole 558										
27-3, 51-54	3.70×10^{-4}	−51[b]	690	1.51×10^{-3}	282	4.08	0.41	8.98×10^{-5}	8.2	Pillow margin
27-3, 123-126	1.81×10^{-3}	−45	405	3.00×10^{-3}	165	1.66	0.41	1.24×10^{-4}	29.2	Pillow interior
28-3, 9-12	4.19×10^{-4}	−20[b]	739	2.18×10^{-3}	372	5.20	0.50	1.13×10^{-4}	7.4	Pillow margin
28-3, 43-47	2.05×10^{-3}	−23	248	4.44×10^{-3}	181	2.17	0.73	2.25×10^{-4}	18.2	Pillow interior
29-2, 138-141	3.63×10^{-3}	+34[b]	541	2.33×10^{-3}	369	0.64	0.68	1.73×10^{-4}	42.0	Pillow interior
29-2, 100-103	1.11×10^{-3}	+29	61%	4.23×10^{-4}	769	0.38		7.08×10^{-5}	31.4	Pillow margin
32-5, 30-33	2.85×10^{-3}	−39	475	2.37×10^{-3}	277	0.83	0.58	1.08×10^{-4}	52.8	Flow interior
32-5, 106-109	1.32×10^{-3}	−42	652	2.04×10^{-3}	359	1.55	0.55	8.32×10^{-5}	31.7	Flow margin
35-2, 71-74	1.82×10^{-4}	−72	80%	3.49×10^{-4}	244	1.92		6.89×10^{-5}	5.3	Pillow margin
35-2, 98-101	2.18×10^{-3}	−54	681	1.53×10^{-3}	362	0.70	0.53	6.08×10^{-5}	71.7	Pillow interior
36-2, 130-133	4.55×10^{-4}	−44	667	1.66×10^{-3}	367	3.65	0.55	8.22×10^{-5}	11.1	Flow margin
36-3, 18-21	7.74×10^{-3}	−51[b]	685	1.52×10^{-3}	321	0.20	0.47	9.00×10^{-5}	172.0	Flow interior
38-1, 56-59	2.34×10^{-3}	−33	444	3.48×10^{-3}	226	1.49	0.51	1.25×10^{-4}	37.4	Pillow margin
38-2, 42-45	3.65×10^{-3}	+32	258	2.71×10^{-3}	182	0.74	0.71	1.70×10^{-4}	42.9	Pillow interior
39-4, 4-7	3.31×10^{-3}	−26	421	2.43×10^{-3}	388	0.73	0.92	1.04×10^{-4}	63.7	Possible flow
39-4, 55-57	1.82×10^{-3}	−26	485	1.40×10^{-3}	285	0.77	0.59	8.40×10^{-5}	43.3	Possible flow
Average	2.20×10^{-3}	−40[c]	528	2.09×10^{-3}	322	1.67	0.58	1.11×10^{-4}	32.1	
Hole 559										
4-1, 115-118	6.40×10^{-4}	−31	651	1.54×10^{-3}	315	2.41	0.48	1.20×10^{-4}	10.7	Pillow interior
4-1, 133-136	6.87×10^{-4}	−37	460	1.82×10^{-3}	292	2.64	0.63	1.34×10^{-4}	10.3	Pillow margin
6-2, 20-23	5.34×10^{-4}	−30[b]	804	1.27×10^{-3}	323	2.40	0.40	1.10×10^{-4}	9.7	Pillow interior
6-2, 50-53	1.77×10^{-4}	+27[b]	55%	2.73×10^{-3}	267	15.4		1.08×10^{-4}	3.3	Pillow margin
Average	5.10×10^{-4}	33[c]	638[d]	1.84×10^{-3}	299	5.64	0.50	1.18×10^{-4}	8.5	
Hole 561										
2-2, 15-18	2.35×10^{-3}	−62	303	4.09×10^{-3}	283	1.74	0.93	3.39×10^{-4}	13.9	Pillow margin
2-2, 45-48	3.31×10^{-3}	−59	345	3.61×10^{-3}	299	1.09	0.87	3.50×10^{-4}	18.9	Pillow interior
3-1, 67-70	3.07×10^{-3}	−53	346	3.86×10^{-3}	312	1.26	0.90	3.19×10^{-4}	19.2	Massive flow
3-2, 42-45	1.37×10^{-3}	−44[b]	341	3.53×10^{-3}	257	2.58	0.75	2.7×10^{-4}	10.1	Massive flow
Average	2.53×10^{-3}	−55	334	3.77×10^{-3}	288	1.67	0.86	3.20×10^{-4}	15.5	
Hole 562										
1-2, 27-30	8.81×10^{-4}	−33	513	7.81×10^{-3}	100	8.90	0.19	8.49×10^{-4}	2.1	Pillow margin
1-2, 61-64	2.43×10^{-3}	−50	363	3.78×10^{-3}	210	1.56	0.58	2.00×10^{-4}	24.3	Pillow interior
4-2, 38-41	1.67×10^{-3}	−36	353	4.44×10^{-3}	131	2.66	0.37	2.94×10^{-4}	11.4	Massive flow
4-3, 72-75	1.85×10^{-3}	−35	132	3.83×10^{-3}	86	2.07	0.65	3.47×10^{-4}	10.7	Flow margin
4-3, 129-132	6.90×10^{-4}	−30	478	3.20×10^{-3}	309	4.64	0.65	1.77×10^{-4}	7.8	Pillow margin
4-4, 30-33	2.19×10^{-3}	−31	526	2.71×10^{-3}	357	1.24	0.68	8.39×10^{-5}	52.0	Pillow interior
5-2, 78-81	2.14×10^{-3}	−33	414	5.03×10^{-3}	154	2.35	0.37	4.51×10^{-4}	9.5	Flow margin
5-2, 104-107	1.13×10^{-3}	−26	282	3.61×10^{-3}	232	3.19	0.82	3.28×10^{-4}	6.9	Flow interior
6-3, 19-22	3.13×10^{-3}	−31	736	3.20×10^{-3}	685	1.02	0.93	9.27×10^{-5}	67.5	Pillow margin
6-3, 61-64	2.39×10^{-3}	−29	505	2.85×10^{-3}	346	1.19	0.69	9.33×10^{-5}	51.2	Pillow interior
Average	1.85×10^{-3}	−33	430	4.05×10^{-3}	261	2.88	0.59	2.92×10^{-4}	24.3	
Hole 563										
24-1, 3-6	1.96×10^{-3}	+42	315	4.94×10^{-3}	207	2.52	0.66	4.27×10^{-4}	9.2	Pillow interior
24-1, 33-36	4.96×10^{-3}	+47	271	4.86×10^{-3}	327	0.98	1.21	3.43×10^{-4}	28.9	Pillow margin
Average	3.46×10^{-3}	+45	293	4.90×10^{-3}	267	1.75	0.94	3.85×10^{-4}	19.1	
Hole 564										
1-3, 4-7	1.94×10^{-3}	+10	549	1.29×10^{-3}	319	0.66	0.58	1.33×10^{-4}	29.2	Pillow interior
1-1, 46-47	3.77×10^{-3}	−5	379	4.34×10^{-3}	296	1.15	0.78	1.82×10^{-4}	41.4	Pillow margin
5-3, 93-96	1.93×10^{-3}	+26	457	6.01×10^{-3}	182	3.11	0.40	1.95×10^{-4}	19.8	Flow interior
5-3, 44-47	1.52×10^{-3}	+14	444	3.37×10^{-3}	351	2.22	0.79	1.82×10^{-4}	16.7	Flow margin
6-2, 104-107	5.15×10^{-3}	+9	129	8.11×10^{-3}	195	1.57	1.51	1.04×10^{-3}	10.6	Pillow margin
6-2, 50-53	2.30×10^{-3}	+28	554	4.72×10^{-3}	199	2.05	0.36	1.88×10^{-4}	24.5	Pillow interior
8-2, 75-78	3.88×10^{-3}	−20	240	4.94×10^{-3}	154	1.27	0.64	2.88×10^{-4}	26.9	Flow interior
9-2, 71-74	1.84×10^{-3}	+15	326	5.94×10^{-3}	326	3.23	1.0	1.63×10^{-4}	22.6	Flow margin
Average	2.78×10^{-3}	+17[c]	385	4.84×10^{-3}	253	1.91	0.76	2.94×10^{-4}	24.0	

Note: J_N is the natural remanent magnetization; I is the inclination; MDF_N is median demagnetizing field for NRM; J_A is the anysteretic remanent magnetization (ARM) value; MDF_A is the median demagnetizing field for ARM: χ_0 is weak field susceptibility; and Q is the Koenigsberger ratio ($J_N/0.5X_O$).

[a] % in this column indicates the remanence remaining at 1000 Oe.

[b] Multicomponent magnetization.

[c] Excludes values with different polarity than the majority of samples.

[d] Excludes samples wih MDF > 1000 Oe.

APPENDIX B
Intrinsic Properties

Core-Section (interval in cm)	J_s ($emu \cdot g^{-1}$)	J_r ($emu \cdot g^{-1}$)	H_c (Oe)	H_{cr} (Oe)	$\frac{J_r}{J_s}$	$\frac{H_{cr}}{H_c}$	χ_p ($emu \cdot g^{-1} \cdot Oe^{-1} \cdot 10^{-5}$)	T_c (°C) Heating	T_c (°C) Cooling	$\frac{J_f}{J_A}$
Hole 556										
5-1, 78–80	1.27×10^{-1}	8.25×10^{-2}	372	463	0.65	1.2	1.59	270	545	10.6
5-1, 111–113	8.95×10^{-2}	6.04×10^{-2}	419	581	0.67	1.4	1.54	315	535	
7-1, 47–49	1.26×10^{-1}	5.79×10^{-2}	198	269	0.46	1.4	1.13	355	590	8.8
7-3, 18–21	1.49×10^{-1}	8.10×10^{-2}	198	238	0.54	1.2	1.36	310	560	6.1
8-2, 6–9	1.11×10^{-1}	5.67×10^{-2}	269	363	0.51	1.35	1.08	380	610	7.3
8-2, 80–83	2.77×10^{-2}	1.26×10^{-2}	175	388	0.45	2.2	1.42	495	560	4.1
9-1, 143–146	1.15×10^{-1}	5.59×10^{-2}	259	363	0.49	1.4	1.32	365	575	8.4
9-1, 127–130	7.86×10^{-2}	4.35×10^{-2}	364	561	0.55	1.5	1.22	365	590	11.7
Average	1.03×10^{-1}	5.63×10^{-2}	282	403	0.54	1.5	1.33	357	571	8.1
Hole 557										
1-1, 46–49	1.47	1.89×10^{-1}	39	91	0.13	2.3	1.45	195		1.0
1-1, 120–123	1.48	2.80×10^{-1}	88	139	0.19	1.6	3.14	350	445	0.3
Average	1.48	2.35×10^{-1}	64	115	0.16	2.0	2.30	273	445	0.7
Hole 558										
27-3, 51–54	1.22×10^{-1}	5.01×10^{-2}	189	297	0.41	1.6	1.16	340	570	6.6
27-3, 123–126	1.83×10^{-1}	9.17×10^{-2}	173	247	0.50	1.4	1.55	265	445	5.0
28-3, 9–12	7.32×10^{-2}	3.66×10^{-2}	298	456	0.50	1.5	1.29	350	565	8.0
28-3, 43–47	1.16×10^{-1}	6.93×10^{-2}	317	398	0.60	1.3	1.45	295	545	5.6
29-2, 138–141	1.11×10^{-1}	6.46×10^{-2}	278	311	0.58	1.1	1.57	320	540	5.1
29-2, 100–103	4.05×10^{-2}	2.02×10^{-2}	431		0.50		1.48	375	570	2.4
32-5, 30–33	1.44×10^{-1}	6.66×10^{-2}	247	399	0.46	1.4	1.38	305	560	7.6
32-5, 106–109	1.03×10^{-1}	5.66×10^{-2}	306	427	0.55	1.4	1.36	295	560	8.2
35-2, 71–74	2.66×10^{-2}	1.51×10^{-2}	428		0.57		1.33	385	580	4.8
35-2, 98–101	1.14×10^{-1}	7.03×10^{-2}	472	636	0.62	1.4	1.46	310	570	6.8
36-2, 130–133	5.33×10^{-2}	3.24×10^{-2}	353	541	0.61	1.5	1.04	360	550	9.9
36-3, 18–21	1.43×10^{-1}	8.76×10^{-2}	411	542	0.61	1.3	1.46	320	580	6.0
38-1, 56–59	1.59×10^{-1}	7.41×10^{-2}	172	238	0.47	1.4	1.41	315	555	5.1
38-2, 42–45	2.15×10^{-1}	9.95×10^{-2}	202	275	0.46	1.4	1.41	295	530	4.7
39-4, 4–7	9.64×10^{-2}	4.92×10^{-2}	244	339	0.51	1.4	1.10	350	555	8.8
39-4, 55–57	8.35×10^{-2}	4.76×10^{-2}	284	398	0.57	1.4	1.20	320	580	11.9
Average	1.11×10^{-1}	5.82×10^{-2}	300	389	0.53	1.4	1.35	325	553	6.3
Hole 559										
4-1, 115–118	1.15×10^{-1}	5.97×10^{-2}	283	413	0.52	1.5	1.42	310	580	9.5
4-1, 133–136	8.44×10^{-2}	4.62×10^{-2}	309	463	0.55	1.5	0.93	315	560	10.8
6-2, 20–23	7.82×10^{-2}	4.86×10^{-2}	391	594	0.62	1.5	1.34	365	590	10.0
6-2, 50–53	5.92×10^{-2}	3.33×10^{-2}	281	466	0.56	1.7	1.16	395	580	11.2
Average	8.42×10^{-2}	4.70×10^{-2}	316	484	0.56	1.6	1.21	346	578	10.4
Hole 561										
2-2, 15–18	2.80×10^{-1}	1.33×10^{-1}	230	278	0.48	1.2	1.65	375	545	2.7
2-2, 45–48	3.16×10^{-1}	1.37×10^{-1}	272	384	0.43	1.4	1.62	335	570	4.2
3-1, 67–70	2.93×10^{-1}	1.40×10^{-1}	248	330	0.48	1.3	1.49	340	(a)	
3-2, 42–45	3.06×10^{-1}	1.37×10^{-1}	242	338	0.45	1.4	1.70	305	575	4.7
Average	2.99×10^{-1}	1.37×10^{-1}	248	333	0.46	1.3	1.62	339	563	3.9
Hole 562										
1-2, 27–30	5.80×10^{-1}	1.70×10^{-1}	106	194	0.29	1.8	2.07	205	(a)	1.1
1-2, 61–64	2.55×10^{-1}	1.20×10^{-1}	211	278	0.47	1.3	1.83	290	565	5.8
4-2, 38–41	2.54×10^{-1}	1.04×10^{-1}	172	230	0.41	1.3	1.49	305	520	
4-3, 72–75	3.83×10^{-1}	1.30×10^{-1}	145	217	0.34	1.5	1.96	270	550	4.2
4-3, 129–132	6.03×10^{-2}	2.49×10^{-2}	188	413	0.41	2.2	1.43	525	570	4.5
4-4, 30–33	1.31×10^{-1}	8.62×10^{-2}	304	467	0.66	1.3	1.50	260	545	8.6
5-2, 78–81	5.03×10^{-1}	1.16×10^{-1}	89	169	0.23	1.9	1.93	260		
5-2, 104–107	2.99×10^{-1}	8.80×10^{-2}	139	217	0.29	1.6	1.47	370	(a)	1.4
6-3, 19–22	1.32×10^{-1}	8.90×10^{-2}	517	728	0.67	1.4	1.71	315	550	3.9
6-3, 61–64	1.15×10^{-1}	7.53×10^{-2}	388	513	0.66	1.3	1.49	285	530	6.3
Average	2.71×10^{-1}	1.00×10^{-1}	226	343	0.44	1.6	1.69	309	547	4.5
Hole 563										
24-1, 3–6	3.24×10^{-1}	1.32×10^{-1}	173	238	0.41	1.4	1.35	415	575	3.4
24-1, 33–36	2.66×10^{-1}	1.05×10^{-1}	236	331	0.40	1.4	1.38	415		3.3
Average	2.95×10^{-1}	1.19×10^{-1}	205	285	0.41	1.4	1.37	415	575	3.4
Hole 564										
1-3, 4–7	1.38×10^{-1}	7.41×10^{-2}	313	472	0.54	1.5	1.43	375	580	9.2
1-1, 46–49	2.80×10^{-1}	1.42×10^{-1}	255	334	0.51	1.3	1.66	340	555	5.3
5-3, 93–96	2.68×10^{-1}	1.35×10^{-1}	188	233	0.51	1.2	1.68	305	560	6.2
5-3, 44–47	1.78×10^{-1}	7.52×10^{-2}	214	336	0.42	1.6	1.39	380	575	5.3
6-2, 104–107	4.79×10^{-1}	1.05×10^{-1}	88	159	0.22	1.8	1.38	505	575	1.3
6-2, 50–53	2.61×10^{-1}	1.24×10^{-1}	191	259	0.48	1.4	1.75	295	550	5.4
8-2, 75–78	4.76×10^{-1}	1.99×10^{-1}	145	191	0.42	1.3	2.21	285	560	3.6
9-2, 71–74	3.11×10^{-2}	1.48×10^{-2}	227	373	0.48	1.6	0.54	350	560	14.7
9-3, 18–21	1.92×10^{-1}	6.81×10^{-2}	231	473	0.36	2.1	1.72	575	555	1.2
Average	2.56×10^{-1}	1.04×10^{-1}	206	314	0.44	1.5	1.53	357	563	5.8

Note: J_s is saturation magnetization; J_r is saturation remanence; H_c is coercivity; H_{cr} is remanent coercivity; χ_p is paramagnetic susceptibility; T_c is Curie temperature; J_f is J_s after inversion; J_i is J_s before inversion. The heating value of T_c is that before inversion; the cooling value follows heating to about 620°.

[a] T_c too low to be measured accurately.